nature chemical biology

ARTICLE

PUBLISHED ONLINE: 31 OCTOBER 2010 | DOI: 10.1038/NCHEMBIO.466

Ultrasensitive *in situ* visualization of active glucocerebrosidase molecules

Martin D Witte[1,7], Wouter W Kallemeijn[2,7], Jan Aten[3], Kah-Yee Li[1], Anneke Strijland[2], Wilma E Donker-Koopman[2], Adrianus M C H van den Nieuwendijk[1], Boris Bleijlevens[2], Gertjan Kramer[2,4], Bogdan I Florea[1], Berend Hooibrink[5], Carla E M Hollak[6], Roelof Ottenhoff[2], Rolf G Boot[2], Gijsbert A van der Marel[1], Herman S Overkleeft[1]* & Johannes M F G Aerts[2]*

Deficiency of glucocerebrosidase (GBA) underlies Gaucher disease, a common lysosomal storage disorder. Carriership for Gaucher disease has recently been identified as major risk for parkinsonism. Presently, no method exists to visualize active GBA molecules *in situ*. We here report the design, synthesis and application of two fluorescent activity-based probes allowing highly specific labeling of active GBA molecules *in vitro* and in cultured cells and mice *in vivo*. Detection of *in vitro* labeled recombinant GBA on slab gels after electrophoresis is in the low attomolar range. Using cell or tissue lysates, we obtained exclusive labeling of GBA molecules. We present evidence from fluorescence-activated cell sorting analysis, fluorescence microscopy and pulse-chase experiments of highly efficient labeling of GBA molecules in intact cells as well as tissues of mice. In addition, we illustrate the use of the fluorescent probes to study inhibitors and tentative chaperones in living cells.

The lysosomal hydrolase GBA hydrolyzes glucosylceramide[1,2]. This ubiquitously expressed enzyme is initially synthesized as a 519-residue protein that cotranslationally acquires four N-linked glycans. After the removal of its signal peptide, GBA undergoes no further post-translational proteolytic modification and does not acquire mannose-6-phosphate moieties in the Golgi apparatus. The expression of disease in individuals with a defective GBA is remarkably heterogeneous. Substantial deficiency results in Gaucher disease, and recently carriership has been recognized as major risk for parkinsonism[2,3]. The manifestation of Gaucher disease is highly variable, ranging from the common non-neuronopathic (type 1) variant to more severe manifestations with lethal neurological complications (type 2 and 3 variants) and extreme cases with abnormalities in skin permeability (so-called collodion babies)[2]. The marked phenotypic heterogeneity is only partly explained by differences in underlying mutations in the GBA gene. The heteroallelic presence of N370S GBA, the most frequent mutation in Caucasian individuals, protects against a neuronopathic manifestation, whereas homozygosity for L444P GBA is associated with severe neurological symptoms[2]. Several studies have indicated that the relationship between GBA genotype and Gaucher phenotype is not very strict[4]. Even phenotypic heterogeneity among identical twins has been reported, suggesting that additional factors influence the *in situ* residual activity of GBA[5].

Two treatments for Gaucher disease presently exist: enzyme replacement therapy and substrate reduction therapy. Enzyme replacement therapy is based on chronic intravenous administration of recombinant GBA (imiglucerase; trade name: Cerezyme)[6,7]. Substrate reduction therapy is based on chronic oral administration of *N*-butyldeoxynojirimycin, an inhibitor of the enzyme glucosylceramide synthase, which catalyzes the formation of glucosylceramide[8,9]. More recently, an alternative approach has received considerable attention, so-called chaperone therapy. Common in Gaucher patients are mutant forms of GBA that show impaired folding and retention in the endoplasmic reticulum, ultimately resulting in elimination via the ubiquitin-proteasome system, a process known as ER-associated degradation (ERAD)[10–15]. Studies have investigated small compounds, designated 'chemical chaperones', that are able to increase the amount of GBA by stabilizing and/or promoting folding of the enzyme. One extensively studied example is isofagomine (**1**), which is a potent competitive inhibitor interacting with the catalytic pocket[16–20]. Beneficial effects on the amount and lysosomal localization of mutant GBA forms in cultured cells have been reported for isofagomine, but the assays used to demonstrate increased degradative capacity have been quite artificial: cells are exposed to high concentrations of fluorogenic substrate at acidic pH (see, for example, ref. 17). It is not likely that exposing cells to low pH and millimolar concentrations of 4-methylumbelliferyl β-D-glucopyranoside for a prolonged period reflects faithfully the *in situ* ability of the enzyme to degrade glucosylceramide. Pharmacologic chaperones like isofagomine will only exert a positive clinical effect at a particular dose range: their concentration should be sufficiently high to promote folding of the enzyme in the endoplasmic reticulum to increase transport to lysosomes, whereas the concentration in lysosomes should also be sufficiently low to prevent marked inhibition of catalytic activity. The present lack of a suitable method for specific visualization of active GBA molecules is a major limitation in research on Gaucher disease and parkinsonism, as well as the development of new therapies. For this reason, we embarked on the development of such a method using activity-based labeling. The catalytic mechanism of GBA, a retaining glucosidase, has been elucidated in detail[21,22]. Briefly, unprotonated Glu340 in GBA performs the initial nucleophilic attack on the substrate, forming a covalently linked enzyme-substrate intermediate.

[1]Leiden Institute of Chemistry, Leiden University, Leiden, The Netherlands. [2]Department of Medical Biochemistry, Academic Medical Center, Amsterdam, The Netherlands. [3]Department of Pathology, Academic Medical Center, Amsterdam, The Netherlands. [4]Mass Spectrometry, Swammerdam Institute for Life Sciences, Amsterdam, The Netherlands. [5]Department of Cell Biology and Histology, Academic Medical Center, Amsterdam, The Netherlands. [6]Department of Endocrinology and Metabolism, Academic Medical Center, Amsterdam, The Netherlands. [7]These authors contributed equally to this work. *e-mail: h.s.overkleeft@chem.LeidenUniv.nl or j.m.aerts@amc.uva.nl

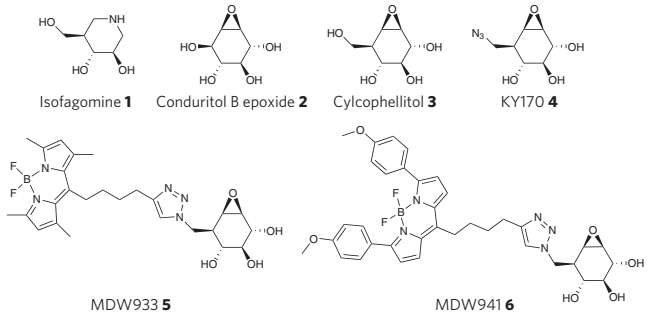

Figure 1 | Structures of isofagomine, CBE, cyclophellitol, KY170, MDW933 and MDW941.

Epoxides like conduritol B epoxide (**2**, CBE) and cyclophellitol (**3**) (**Fig. 1**) form first a noncovalent inhibitor–enzyme complex that then reacts with the Glu340 carboxylate to form a covalent bond, thus acting as irreversible inhibitors. Cyclophellitol resembles more closely the structure of glucoside substrates and is the more potent irreversible inhibitor of the two[23]. We capitalized on this by grafting boron dipyrromethene (BODIPY) fluorophores on to the cyclophellitol core (**Fig. 1**). We here demonstrate highly efficient labeling of GBA *in situ* by these probes and reveal their use in monitoring GBA activity in Gaucher fibroblasts.

RESULTS

Design and synthesis of activity-based probes

We synthesized cyclophellitol (ref. 24) and 8-deoxy-8-azidocyclophellitol (**4**, KY170) (**Fig. 1**; for synthesis see **Supplementary Results**) and tested their inhibitory properties toward recombinant GBA (Genzyme). Cyclophellitol and its azido analog KY170 were found to be far more potent inhibitors of GBA than CBE. Click ligating BODIPY moieties to KY170 gave fluorescent inhibitors MDW933 (**5**) and MDW941 (**6**) (**Fig. 1**; for synthesis, see **Supplementary Results**). Examination of the inhibitory properties revealed that MDW933 and MDW941 were comparably potent as irreversible inhibitors, being markedly superior to CBE and even surpassing cyclophellitol and KY170. The apparent half-maximal inhibitory concentration (IC_{50}) values of both fluorescent compounds (MDW933: $IC_{50} = 1.24 \pm 0.04$ nM; MDW941: $IC_{50} = 1.94 \pm 0.08$ nM) were very similar, being about 100- and 1,000-fold lower than those of cyclophellitol and KY170 ($IC_{50} = 0.15 \pm 0.009$ μM and 0.12 ± 0.004 μM, respectively) and CBE ($IC_{50} = 9.49 \pm 0.042$ μM). We determined next the inhibition constants—the K_i (the equilibrium constant for initial binding), the rate constant (k_i) and the relative rate constant k_i/K_i—for CBE, cyclophellitol, KY170, MDW933 and MDW941 using a continuous substrate release assay (see **Supplementary Fig. 1** for progress curves). A general trend that we observed for the equilibrium constant for initial binding was that increased hydrophobicity resulted in decreased K_i values (**Table 1**). Comparison of relative rate constants demonstrated that the fluorescent probes inhibited GBA 22-, 34- and 4,300-fold better than KY170, cyclophellitol and CBE.

The affinity of MDW933 and MDW941 for GBA was unexpectedly high. For a better understanding of this finding, we performed molecular docking analysis using the GBA crystal structure (PDB: 2V3E)[25]. The docking model revealed that at minimum free energy of the simulated enzyme–ligand complex, both fluorescent probes efficiently bound to the GBA active site. Tight fitting of the BODIPY moiety in a hydrophobic pocket near the position in the active site where the 6′-hydroxyl of its natural substrate would reside appears to contribute to the binding. In this orientation, the epoxide was positioned 3 Å away from Glu340, close enough to allow nucleophilic addition of the Glu340 carboxylate (**Supplementary Fig. 2**). The calculations yielded minimum free energy values that were significantly lower for the hydrophobic fluorescent probes MDW933 and MDW941 (−8.1 kcal mol^{-1} and −8.4 kcal mol^{-1}) than for KY170 (−5.2 kcal mol^{-1}), explaining their superior inhibitory properties. Notably, when we compared the crystal structure of GBA (PDB: 2VT0) with the modeled enzyme structure (PDB: 2V3E) with CBE or MDW933 (**Supplementary Fig. 2**), the cyclitol moiety did not completely overlap with that of CBE covalently bound to 2VT0. The intrinsic differences in structure coordinates between the crystal structures, as well as the comparison of the positioning of CBE and MDW933 before the prenucleophilic attack with the already covalently bound state of CBE, could have caused this discrepancy. The presence of the latter was likely enough to physically alter the local protein structure.

Table 1 | Binding constants of the inhibitors

	k_i (min^{-1})	K_i (μM)	k_i/K_i (μM^{-1} min^{-1})
CBE **2**	0.217 ± 0.026	53 ± 10.8	0.004
Cyclophellitol **3**	0.078 ± 0.010	0.152 ± 0.026	0.514
KY170 **4**	0.035 ± 0.003	0.044 ± 0.007	0.794
MDW933 **5**	0.127 ± 0.024	0.007 ± 0.002	17.76
MDW941 **6**	0.208 ± 0.063	0.008 ± 0.003	25.10

K_i and k_i values were calculated as described in the **Supplementary Results** and **Methods** and reported with s.e.m.

In vitro labeling of GBA with the fluorescent ABPs

To examine labeling of recombinant GBA by MDW933 and MDW941, we incubated the enzyme for 30 min at 37 °C with mixtures of both probes at pH 5.2, with 0.2% (w/v) taurocholate and 0.1% (v/v) Triton X-100, an optimal condition for enzymatic activity and activity-based labeling. After the incubation, we resolved the protein preparations with SDS-PAGE and analyzed the labeled proteins by fluorescence scanning of the slab gel on a Typhoon Variable Mode Imager (**Fig. 2a**). Labeled recombinant GBA migrated at the expected mass of 57 kDa. At equimolar concentration of MDW933 and MDW941 (100 nM), both probes bound the enzyme equally well. Thus, labeling of GBA with both probes was comparable, as expected given their similar inhibition constants. Boiling of the samples before electrophoresis had no impact on the detection of the fluorescently labeled protein on the slab gel, indicating that the probe was firmly attached. The presence of reducing agent also did not affect the covalent binding of the probes.

We determined the sensitivity of detection of labeled GBA by incubating 2 pmol GBA with an excess of MDW933 (20 nmol at 1 mM concentration) for 1 h at 37 °C and subsequent titration of the amount applied on the gel (**Fig. 2b**). We could detect as little as 20 attomol GBA by fluorescence scanning. Next, we incubated equal amounts of GBA (2 pmol) for 30 min with decreasing amounts of MDW933 and applied all protein to a gel. Incubation with as little as 20 attomol of probe resulted in detectable GBA on the slab gel (**Fig. 2b**). Apparently, nearly all of the probe had been covalently bound to recombinant GBA, consistent with its high affinity for binding. These experiments indicated that ultrasensitive detection of GBA was feasible on slab gels following *in vitro* labeling with the fluorescent probes **5** and **6**.

As a next step, we analyzed the site of binding of the probe on GBA using a competition assay. Prior to labeling with MDW933, we incubated recombinant GBA with 2 mM CBE for 30 min (**Fig. 2c**). Preincubation with CBE, shown via crystallography to bind Glu340 (ref. 26), blocked labeling completely. Similarly, we also noticed competition with labeling by the competitive inhibitor AMP-DNM (**7**) (**Fig. 2c**)[27]. These results from competition experiments indicated that indeed the probe was bound in the catalytic center of GBA. We unambiguously identified the site of binding of KY170 and MDW933 by mass spectrometry. Using tryptic digestion and

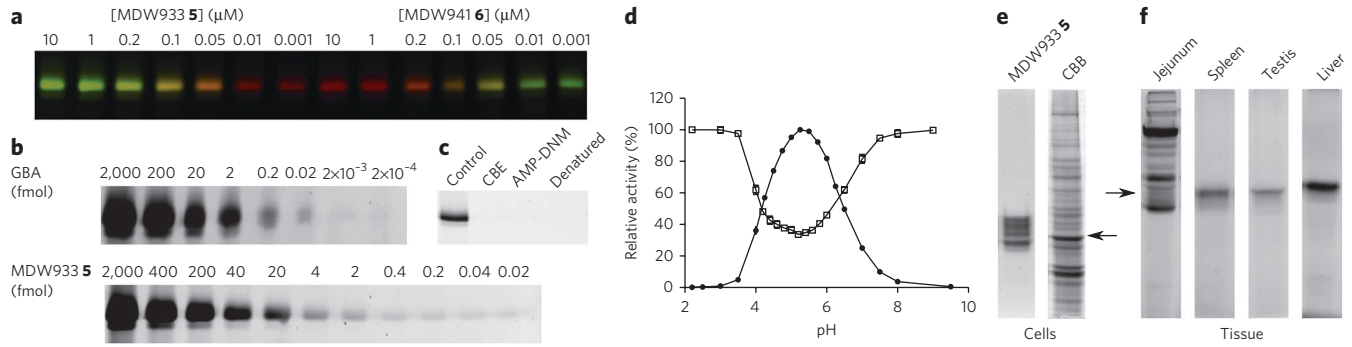

Figure 2 | *In vitro* labeling of GBA with MDW933 and MDW941. (**a**) Labeling of recombinant GBA (Cerezyme) with mixtures of MDW933 and MDW941 detected on slab gel. Left: labeling with the indicated amount of MDW933 in the presence of 100 nM MDW941. Right: labeling with the indicated amount of MDW941 in the presence of 100 nM MDW933. (**b**) Sensitivity of detection and labeling. Upper panel: Cerezyme (2 pmol) was incubated with an excess of MDW933 (1 mM) and dilutions applied on gel. Lower panel: Cerezyme (2 pmol) was incubated with a decreasing amount of MDW933. (**c**) Activity of Cerezyme (2 pmol) was blocked by incubating with CBE (2 mM) or AMP-DNM (2 mM) or by boiling in 1% (w/v) SDS before labeling with MDW933. (**d**) Effect of the pH on inhibition and enzymatic activity. The activity of GBA was determined at various pH values, normalized for the activity at pH 5.2 and plotted (circles). Inhibition by MDW933 was examined at the same pH ranges (open squares). Data represent mean values ± s.d. (**e**) Fluorescent labeling of GBA in homogenates of RAW cells using MDW933 (100 nM) (7.5% SDS-PAGE gel). Proteins were detected by fluorescence imaging (left lane) and Coomassie Brilliant Blue (CBB) staining (right lane). (**f**) Fluorescent labeling of mouse tissue lysates exposed to MDW933 (100 nM) (10% SDS-PAGE gel). Arrows indicate the molecular weight of Cerezyme. For uncut gels, see **Supplementary Figure 11**.

LC-MS/MS, we detected active site fragments of GBA that showed a shift in mass coinciding with binding of KY170 to Glu340 (**Supplementary Fig. 3**). A similar experiment with MDW933 did not render detectable tryptic fragments of interest, most likely because the attachment of the hydrophobic moieties impaired ionization. We circumvented this complication by treating GBA labeled with MDW933 with hydroxylamine before tryptic digestion. This released the probe from GBA and concomitantly converted the modified residue into a hydroxamic acid. The outcome of this experiment demonstrated that MDW933 also bound covalently to Glu340 (**Supplementary Fig. 3**).

Enzymatically active GBA molecules are a prerequisite for labeling with the probe, as demonstrated by the lack of labeling of GBA that had been denatured by boiling (**Fig. 2c**). The same conclusion could be drawn from the pH dependence of irreversible inhibition of GBA by the fluorescent probes. It exactly coincided with the pH profile of enzymatic activity toward 4-methylumbelliferyl β-D-glucopyranoside (**Fig. 2d**).

Labeling of GBA in cell and tissue extracts

To determine the labeling specificity of both fluorescent probes, we incubated homogenates of cultured cells and mouse tissues with 100 nM green fluorescent MDW933 for 30 min at 37 °C and analyzed the preparation with SDS-PAGE. In the case of homogenates of cultured RAW cells, fluorescence scanning showed exclusive labeling of GBA by MDW933. The various GBA forms, with molecular mass ranging 58–66 kDa owing to glycan differences, were visualized (**Fig. 2e**). With several other cell types such as HepG2 cells, COS cells and human fibroblasts, we obtained similar results (**Supplementary Fig. 4**). Furthermore, red fluorescent MDW941 also labeled GBA selectively in RAW cells (**Supplementary Fig. 4**). It was striking that incubation of cell lysates with the probes did not result in fluorescent labeling of other cellular proteins. Furthermore, we observed very similar results—that is, highly specific labeling of GBA—using lysates of mouse tissues (**Fig. 2f**). Homogenates of mouse intestine were the only exception, most likely owing to labeling of high–molecular weight lactase and fragments thereof. Lactase (lactase-phloridzin hydrolase: LPH) is known to covalently bind CBE[28], and we therefore reasoned that MDW933 may also irreversibly inhibit lactase activity. This was indeed the case: incubation for 30 min with 1 mM of MDW933 resulted in ~90% inhibition of lactase activity. Next, we demonstrated that a high concentration of lactose (250 mM) reduced markedly (>90%) the labeling of the high–molecular weight protein in the intestinal fraction while leaving labeling of GBA practically unaltered (**Supplementary Fig. 5**).

In situ labeling of GBA in cultured cells

We investigated whether labeling of GBA in intact cells was also feasible. For this purpose we added MDW933 or MDW941 to the culture medium at a concentration of 5 nM. At different time points, we harvested the cells and determined the GBA activity in the cell homogenates with artificial substrate (**Fig. 3a**). Even in intact cells, GBA was inactivated by both probes. Apparently, the more hydrophobic MDW941 could more easily reach intracellular GBA. It is presently not clear how exactly the probes enter cellular compartments. It is unlikely that uptake occurred only by endocytosis, given the fast speed of labeling and its occurrence at low temperature at which endocytosis is blocked (**Supplementary Fig. 6**). Direct uptake of the probes, either by diffusion of the amphiphilic structures or by facilitation by transporters, seems most likely.

We studied *in situ* labeling of GBA in cells using fluorescence-activated cell sorting (FACS) analysis. We first preincubated cells in the absence or presence of CBE and subsequently incubated the cells with a subsaturating or an excess amount of the green fluorescent probe **5**. FACS analysis revealed dose-dependent fluorescent labeling of cells and no labeling above background in CBE pretreated cells (**Fig. 3b**). These positive results prompted us to analyze labeling of the cells with fluorescence microscopy (**Fig. 3c–f**). For this purpose, we cultured fibroblasts for 2 h with 5 nM MDW941. We also detected GBA protein by indirect immunofluorescence using the specific anti-GBA monoclonal antibody 8E4 (ref. 29). Using multispectral image analysis, we could specifically distinguish the respective fluorescent emission spectra (**Fig. 3d–e**) from autofluorescent background (**Fig. 3c**). The intracellular pattern of labeling with MDW941 showed an almost complete overlap with the detection of GBA by monoclonal antibody 8E4 using this method (**Fig. 3f**).

As probes with a hydrophobic BODIPY moiety might nonspecifically be retained in membranes, in particular the plasma membrane, we studied this possibility more closely. First, we cultured fibroblasts obtained from a Gaucher patient homozygous for the RecNCI GBA mutation (a mutation resulting in premature degradation of GBA by

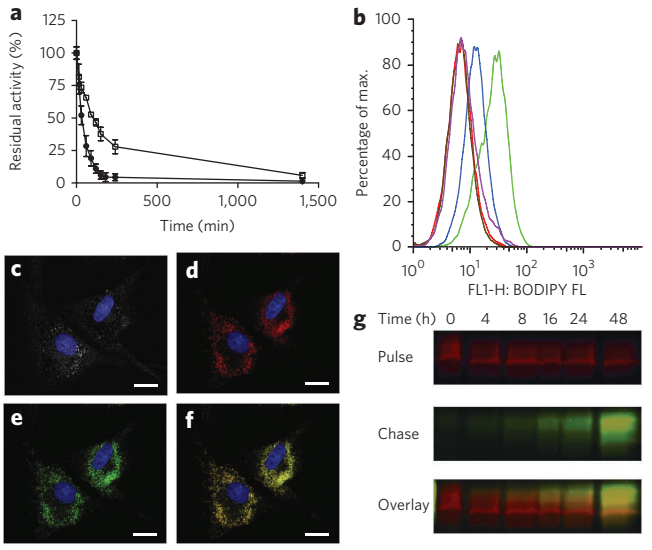

Figure 3 | *In situ* labeling of glucocerebrosidase. (**a**) Inactivation of GBA by MDW933 (squares) and MDW941 (circles) *in situ*. Fibroblasts incubated with the probes (5 nM) for the indicated time were homogenized, and residual activity was determined with 4-methylumbelliferyl β-D-glucopyranoside. Data represent mean values ± s.d. (**b**) FACS analysis. Cells were treated with 0 nM (red line), 2 nM (blue line) and 10 nM (green line) MDW933 for 300 min. Control cells were pretreated with CBE (0.3 mM) and incubated with 2 nM (brown line) and 10 nM (purple line) MDW933. (**c**–**f**) Representative spectral imaging micrographs of cells labeled with MDW941. (**c**) Autofluorescence (white). (**d**) MDW941 BODIPY fluorescence of GBA (red). (**e**) AlexaFluor488 fluorescence of GBA visualized with monoclonal Ab 8E4 (green). (**f**) Overlay of **d** and **e**. In all pictures, nuclei are stained with DAPI (blue). Scale bar represents 20 μm. (**g**) Pulse-chase experiment. Cells were incubated overnight with 10 nM MDW941 (pulse, upper panel) and then with 10 nM MDW933 for the indicated time (chase, middle panel). Lower panel: overlay of the pulse and the chase. Because of the use of low concentration of MDW933 during the first 8 h of the chase, incomplete labeling of newly formed GBA molecules was accomplished. For uncut gels see **Supplementary Figure 12**.

the proteasome) with MDW941. In contrast to control fibroblasts, the patient's cells did not show labeling in the lysosomal compartment by MDW941 but only in the perinuclear area (**Supplementary Fig. 7**). As expected, immunofluorescence using monoclonal 8E4 showed a lysosomal staining pattern for GBA in the control cells whereas RecNCI cells revealed staining for GBA in the cytosol, most likely because of high levels of ERAD and proteasomal degradation in these cells. Next, we cultured wild-type fibroblasts for 16 h in presence of 3 mM CBE to irreversibly inhibit GBA molecules and block labeling. Subsequent culturing of the cells for 2 h with 5 nM MDW941, again in presence of CBE, rendered perinuclear red BODIPY fluorescence that was distinct from the autofluorescence. Control fibroblasts cultured with MDW941 in the absence of CBE revealed labeling in the lysosomal compartment largely overlapping with the autofluorescence (**Supplementary Fig. 8**). Finally, we synthesized MDW1064 (**8**) and MDW1065 (**9**) as nonreactive analogs of probes MDW933 and MDW941 (see **Supplementary Methods** for structure and synthesis). These control probes did inhibit GBA *in vitro* with IC_{50} values of 41 and 95 μM, respectively. However, inhibition is presumably reversible. After culturing of fibroblasts for 2 h with 5 nM control, MDW1065 resulted in hardly any detectable labeling. In the presence of CBE, MDW1065 only weakly labeled the fibroblasts, in a pattern that may suggest interaction with the cell membrane (**Supplementary Fig. 8**).

To show the versatility of the probes, we performed pulse-chase experiments using cultured cells. For this purpose, we incubated fibroblasts overnight with 10 nM red fluorescent MDW941. Subsequently, we treated the cells with 10 nM of the green fluorescent probe, harvested them at different time points (0–48 h) and subjected aliquots of cell homogenates to gel electrophoresis (see **Fig. 3g** for the lifecycle of GBA as visualized in this manner). It should be noted that GBA pulse labeled with the red fluorescent MDW941 disappeared gradually from the cells with an estimated half-life of about 30 h. The obtained half-life was consistent with the half-life determined previously using conventional pulse-chase labeling with radioactive methionine[10]. During the chase, GBA was increasingly labeled with MDW933, coinciding with formation of new GBA molecules (**Fig. 3g**).

We next studied the labeling of GBA by MDW941 in intact fibroblasts using time-lapse microscopy. Fibroblasts treated with the probe showed very rapid fluorescent labeling of lysosome-like structures (see **Supplementary Video**). With 5 nM MDW941, labeling reached a maximum within 15 min. Even after 100 h of exposure to the compound, cells did not show any signs of apoptosis or toxicity. Finally, we examined the possibility of labeling GBA in mice by intravenously administering 0.1 nmol green fluorescent MDW933 dissolved in phosphate-buffered saline to adult mice. As a control, matched mice received the buffer solution intravenously. After 2 h, we killed the animals, prepared tissue extracts, labeled them with excess red fluorescent MDW941 to visualize unlabeled GBA and subjected them to SDS-PAGE (**Fig. 4** shows the outcome of a typical experiment). In most tissues—here we show lung and liver—MDW933 already labeled a considerable proportion of GBA (**Fig. 4a**). Consistently, in such tissues the probe also irreversibly inhibited a large proportion of GBA in the living mouse (see **Fig. 4b**). An exception in this respect was the brain (**Fig. 4a**), in which MDW933 apparently labeled almost no GBA *in vivo* and GBA was not inactivated. As observed earlier, intestinal fractions showed labeling of proteins of multiple molecular masses (**Fig. 4a**). In addition to GBA, MDW933 clearly labeled other proteins that occur in the intestine in the mouse.

Analysis of Gaucher materials

We investigated labeling of mutant GBA in fibroblasts from a normal individual and from Gaucher donors (a N370S GBA homozygote, a L444P homozygote and a RecNCI homozygote manifesting as collodion Gaucher and almost entirely lacking GBA protein) by treating cell lysates with MDW933 (10 nM) for 1 h and subjecting these to SDS-PAGE. A comparison of cells from a normal subject and from a Gaucher donor homozygous for L444P GBA revealed that the

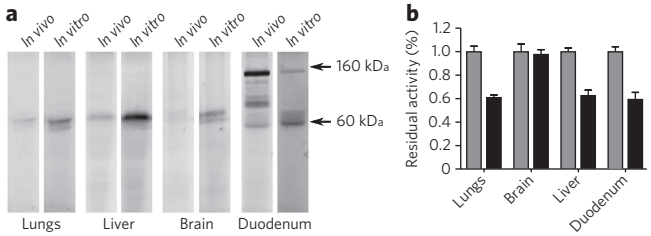

Figure 4 | Labeling of glucocerebrosidase in mice. Adult mice received intravenously 100 pmol green fluorescent MDW933 and were killed after 2 h. (**a**) Tissue lysates were incubated with excess (100 nM) red fluorescent MDW941 for 30 min to label unreacted GBA. *In vivo* labeled GBA (left panels) and *in vitro* labeled GBA (right panels) were visualized separately. For uncut gels, see **Supplementary Figure 13**. (**b**) Residual enzymatic activity in tissues of treated mice (black) was determined with 4-methylumbelliferyl β-D-glucopyranoside substrate and expressed as percentage of the matched control animal (gray). Data represent mean values ± s.d.

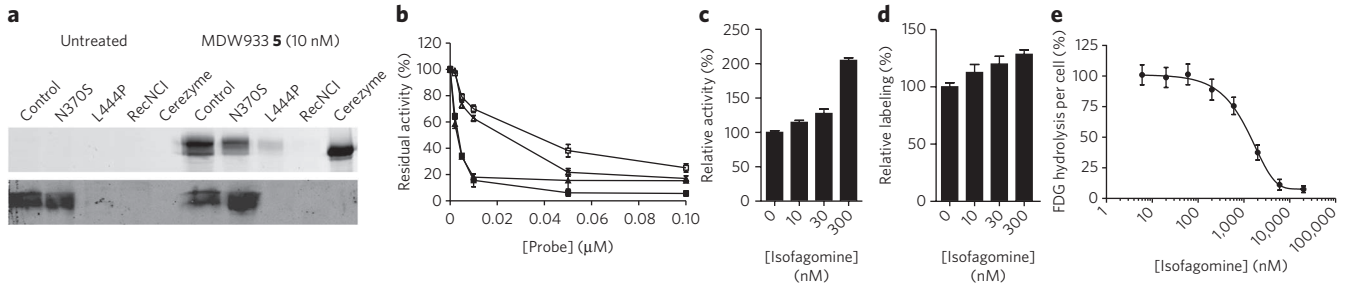

Figure 5 | Labeling of mutant forms of glucocerebrosidase. (**a**) Detection of GBA in Gaucher fibroblasts by labeling of wild-type and homozygous N370S, L444P and RecNCI collodion fibroblast with 10 nM MDW933 for 60 min. GBA was visualized by in-gel fluorescent scanning (top panel) and by western blotting with 8E4 antibody. For uncut gels, see **Supplementary Figure 14**. (**b**) Inactivation curves of MDW933 (open symbol) and MDW941 (solid symbols) in N370S (triangles) and control fibroblasts (squares). Residual activity was determined with 4-methylumbelliferyl β-D-glucopyranoside. Data represent mean values ± s.d. (**c**,**d**) Impact of isofagomine on N370S GBA. In a typical experiment, fibroblasts from the N370S GBA homozygote were incubated with various isofagomine concentrations for 1 week. Data represent mean values ± s.d. (**c**) Relative GBA activity in cell lysates observed with 4-methylumbelliferyl β-D-glucopyranoside assay after incubating. (**d**) Quantification of the fluorescent readout of *in situ* MDW941-labeled GBA activity. (**e**) Relative lysosomal GBA activity observed as hydrolysis of FDG per cell. Fibroblasts were first treated for 20 min with noted concentrations of isofagomine and subsequently incubated with FDG substrate. FDG fluorescence was assessed by FACS analysis. Data represent mean values ± s.d.

amount of L444P GBA was markedly lower in the Gaucher donor (**Fig. 5a**). It is indeed known that L444P GBA undergoes largely premature degradation by ERAD as a result of impaired folding[11]. This phenomenon is far less striking in the case of N370S GBA[10]. Cells from a Gaucher donor homozygous for N370S GBA also showed reduced labeling of GBA but to a lesser extent than cells from a L444P homozygote (**Fig. 5a**). As expected, cells from the RecNCI collodion Gaucher did not show any labeled GBA (**Fig. 5a**). We obtained similar results by analysis of the fibroblast extracts using western blotting and the anti–human GBA antibody 8E4, although the detection limit of this method was far inferior (**Fig. 5a**).

It has been noted that the irreversible inhibition by CBE of N370S GBA is less strong than its inhibition of wild-type GBA[20,30]. We therefore determined inactivation curves of GBA activity in cells of a normal subject and a N370S GBA homozygote (**Fig. 5b**). Notably, MDW933 inactivated GBA activity in wild-type and N370S GBA cells quite similarly. Analysis of GBA in spleen from a Gaucher patient with solely N370S GBA resulted in a similar picture. Labeling of spleen lysates with variable concentrations of MDW933 again resulted in a lower amount of detected GBA protein in that tissue (**Supplementary Fig. 9**).

Impact of isofagomine on N370S GBA in cultured fibroblasts

It has been reported that for cells from N370S GBA homozygotes, prolonged incubation with isofagomine yields an increase in GBA activity[31]. The interaction of isofagomine with the catalytic pocket has been intensely studied, including at the level of crystals[21]. We therefore examined whether incubation of N370S GBA homozygous fibroblasts with isofagomine increased the amount of GBA that can be labeled with fluorescent probes. We cultured cells for 7 d with different concentrations of isofagomine (0, 10, 30 and 300 nM) and subsequently incubated them for 2 h with or without excess MDW941 in the presence of the original concentration of isofagomine. Determination of the activity of GBA in homogenates of cells not treated with MDW941 using 4-methylumbelliferyl β-D-glucopyranoside as substrate revealed a modest isofagomine dose–dependent increase in enzyme activity (seen in **Fig. 5c**). Aliquots from the homogenates of cells labeled with MDW941 were subjected to gel electrophoresis, and the detected fluorescent GBA was quantified. Again we noted a modest dose-dependent increase (**Fig. 5d**), although less marked than the increase in *in vitro* enzyme activity in the homogenates. This discrepancy might be due to concomitant *in situ* stabilization of GBA by isofagomine in combination with competitive inhibition of enzymatic activity. We therefore investigated the effect of isofagomine on GBA activity in the intact cell using 5′-pentafluorobenzoylaminofluorescein-di-β-D-glucoside (FDG) as a substrate. Incubation of fibroblasts with various concentrations of isofagomine for 20 min, subsequent addition of FDG to the medium and quantification of the hydrolysis of FDG by FACS allowed determination of the IC_{50} value of isofagomine in intact cells[32]. The IC_{50} of isofagomine for hydrolysis of FDG was about 1 μM (**Fig. 5e**). Apparently, isofagomine at concentrations >1 mM completely inhibited activity of GBA in intact cells. We studied the reversibility of isofagomine competition for the fluorescent active site labeling. For this purpose, we preincubated recombinant GBA attached to monoclonal antibody 8E4 immobilized to Sepharose beads for 15 min with increasing concentrations of isofagomine at pH 5.2 in the presence of taurocholate (0.2% w/v) and Triton X-100 (0.1% v/v). Prior to labeling with MDW933 (10 nM for 15 min), we either washed or did not wash the bead suspension with the same buffer. Quantification of the labeled GBA on slab gel indicated that the competition of isofagomine for the active site was fully reversible (**Supplementary Fig. 10**).

DISCUSSION

The need for a method allowing visualization of active GBA molecules *in situ* in living cells is evident. It is of importance to understand better what the precise cell and tissue distribution of active GBA molecules is because this may render a better understanding of the pathogenesis of Gaucher disease. Moreover, demonstration of a true increase in active GBA molecules by tentative chaperones is of interest. At present the detection of GBA still relies on the use of antibodies that do not distinguish between active and inactive GBA molecules and can not label enzyme in intact cells. Our search for a suitable probe for activity-based labeling of GBA *in situ* has yielded the desired result. As starting point for the development of such a probe, we selected cyclophellitol, a known potent irreversible inhibitor of GBA that forms a covalent adduct. Next we linked, via a spacer, hydrophobic BODIPY moieties to cyclophellitol. Serendipitously, this led to even more potent irreversible inhibitors. Molecular docking analysis suggested that interaction of the hydrophobic BODIPY moiety in MDW933 and MDW941 with a hydrophobic pocket at the surface of GBA guides the epoxide to a position close to Glu340. This effect may plausibly underlie the remarkable avidity of the two fluorescent compounds as activity-based probes. The labeling of GBA with the fluorescent probes MDW933 and MDW941 seemed to proceed exactly via the expected mechanism for cyclophellitol inhibition of a betaglucosidase[33]. We could indeed demonstrate that labeling could

be blocked with CBE or KY170 and potent competitive inhibitors such as hydrophobic deoxynojirimycines could compete away labeling. Labeling also required the folded enzyme and occurred proportional to enzymatic activity at different pH.

The affinity of both probes for GBA is in fact quite notable: truly ultrasensitive detection of GBA molecules was obtained. The high affinity of the fluorescent probes for GBA offered the opportunity to label the enzyme very specifically. With cell or tissue lysates, exclusive labeling of GBA molecules was observed following electrophoresis. In the case of homogenates of intestine alone we noticed labeling of other proteins, probably fragments of LPH known to covalently interact with CBE. The highly selective labeling of GBA is notable when taking into account the fact that GBA is a very low-abundance protein and constitutes $<10^{-5}$ of all cellular or tissue protein[29]. Another favorable feature of these probes is their ability to enter various cellular compartments. It will be of interest to determine the precise mechanism(s) more closely, although it is already clear that cellular entry seems not to depend on endocytosis. The entry of the probes into living cells allows their use in FACS analysis, and one can perform pulse-chase experiments in intact cells as we have demonstrated. Time-lapse microscopy confirmed that GBA can be labeled very efficiently in intact fibroblasts. We obtained no indications that fluorescent labeling of GBA was toxic to the cells. Initial experiments also indicated that in mice cellular GBA can be labeled with fluorescent cyclophellitol-based compounds. Notably, the brain showed a different picture. Almost no brain GBA was labeled in mice upon intravenous administration of MDW933. This may suggest that MDW933 does not pass the blood-brain barrier or is actively removed from the brain by some P-glycoprotein. The fluorescence features of the green and red fluorescent probes are intrinsically suboptimal for *in situ* imaging of labeled GBA in tissues or whole animals.

The potential applications for the activity-based fluorescent probes MDW933 and MDW941 are substantial. They offer an alternative to antibodies, which are species-specific and can not reach compartmental GBA in intact cells. Moreover, in contrast to antibodies, our probes uniquely label active GBA molecules. One tentative area of application of the fluorescent probes may be diagnosis of Gaucher disease, in particular the demonstration of low amounts of active GBA molecules in fibroblasts or blood cells of patients. This is helpful, as low amounts of active GBA molecules are usually associated with severe, neuronopathic Gaucher disease. Another area of application for these fluorescent probes may be found in the analysis of compounds for their possible inhibitory or chaperone effects. As we demonstrated, the beneficial effect of isofagomine on N370S GBA in cultured fibroblasts could be confirmed with activity-based labeling. This finding is of importance as it implies that at an optimal concentration of isofagomine, occupation of the catalytic center by the competitive inhibitor is *in situ* sufficiently low to allow labeling by the fluorescent probe. In other words, at an appropriate concentration isofagomine indeed increases GBA levels and intralysosomal enzymatic capacity. This finding for isofagomine is not entirely unexpected, as it has been proposed that at the low intralysosomal pH isofagomine interacts less well with β-glucosidases than at neutral pH in the endoplasmic reticulum[34]. Our observations render support for the approach of chaperone therapy, although the dosing of drugs in patients to reach optimal (steady-state) concentrations in various tissues may prove to be a major challenge.

Our approach of selective detection of GBA molecules using fluorescently labeled irreversible inhibitors allows unprecedented, ultrasensitive *in vivo* monitoring of active enzyme molecules. It can be envisioned that the same approach is also feasible for other glycosidases, and another challenging perspective is the future use of the fluorescent probes in living animals. Two approaches can be envisioned. In the first approach the fluorescent probes are used to report on local GBA activity. In the second strategy, recombinant GBA is labeled with the fluorescent probe so that after administration, trafficking of the construct can be monitored in a strategy that is related to another recently reported strategy that uses active site labeling of recombinant and purified GBA with a radiotag[35]. In conclusion, the reported fluorescent activity-based probes offer very versatile research tools to visualize active GBA, ultrasensitively and specifically. This accomplishment may be not only relevant for Gaucher disease but also for parkinsonism.

METHODS

See **Supplementary Methods** for the synthesis of the probes, the methods used to determine the binding constants, molecular docking studies, time-lapse microscopy and mass spectrometric analysis of GBA labeled with KY170 and MDW933.

General methods. Chemicals were obtained from Sigma-Aldrich if not otherwise indicated. Recombinant GBA was obtained from Genzyme. Monoclonal anti-human GBA antibody 8E4 was produced from hybridoma cells as described earlier[36]. Gaucher patients were diagnosed on the basis of reduced GBA activity and demonstration of an abnormal genotype[37]. Fibroblasts were obtained with consent from donors. Cell lines were cultured in HAMF12-DMEM medium (Invitrogen) supplied with 10% (v/v) FBS.

Enzyme activity assays. Activity of GBA was measured at 37 °C with 4-methylumbelliferyl β-D-glucopyranoside as substrate as reported previously. To determine the IC_{50} value, the inhibitors were preincubated for 30 min with the enzyme before addition of the substrate mixture. The incubation mixture contained 3 mM fluorogenic substrate, 0.2% (w/v) sodium taurocholate and 0.1% (v/v) Triton X-100 in 150 mM McIlvaine buffer, pH 5.2. After stopping the incubation with excess NaOH-glycine (pH 10.3), we measured fluorescence with a fluorimeter LS 30 (Perkin Elmer) using λ_{ex} 366 nm and λ_{em} 445 nm. Activity of lactase was quantified by measuring liberated glucose from lactase[38]. *In vivo* activity of GBA in cells was measured using FDG as substrate and FACS[32].

Gel electrophoresis and fluorescence scanning. Electrophoresis in sodium dodecylsulfate containing either 7.5% or 10% polyacrylamide gels was performed as earlier described[29]. Wet slab gels were scanned on fluorescence using the Typhoon Variable Mode Imager (Amersham Biosciences) using λ_{ex} 488 nm and λ_{em} 520 nm (bandpass 40) for green fluorescent MDW933 and λ_{ex} 532 nm and λ_{em}610 nM (bandpass 30) for red fluorescent MDW941.

Fluorescence microscopy and multispectral imaging. Fibroblasts were cultured on glass slides. Cells were incubated with MDW941 (5 nM) or control probe MDW1065 (5 nM) for 2 h. Next, cells were washed, fixed with 3% (v/v) paraformaldehyde in PBS for 15 min, washed and incubated first with 0.05% (w/v) saponine for 15 min, next with 0.1 mM NH_4Cl in PBS for 10 min and then with 3% (w/v) bovine serum albumin in PBS for 1 h. Next, the slides were incubated with anti-GBA monoclonal antibody 8E4 (1:500). Bound mouse monoclonal antibody was visualized with a secondary antibody conjugated with AlexaFluor488. Nuclei were stained with DAPI. Cells were examined using epifluorescence microscopy (Leica DM5000B) with an HCX PL APO ×63 1.40–0.60 oil immersion objective. Filter blocks used were A4 (360/40 nm band pass excitation, 400 nm dichromatic mirror, 470/40 nm band pass suppression) for DAPI, L5 (480/40 nm band pass excitation, 505 nm dichromatic mirror, 527/30 nm band pass suppression) for AlexaFluor488 and N2.1 (515–560 nm band pass excitation, 580 nm dichromatic mirror, 590 nm long pass suppression) for MDW941 and MDW1065. Analysis was performed with multispectral imaging using a Nuance N-MSI-420-20 camera with Nuance 2.10 software (Cambridge Research & Instrumentation). Data sets were acquired at 440–500 nm for A4, 500–580 nm for L5, and 580–720 nm for N2.1 filter blocks, each at 10 nm intervals. In each experiment, nonlabeled control cells were imaged to define the autofluorescence spectral library. Spectral libraries for DAPI, AlexaFluor488 and MDW941 or MDW1065, each obtained from single-stained cells, were used to unmix the triple staining patterns into the individual components and separate these from autofluorescence. Nuance software was used to construct composite images.

Fluorescence-activated cell sorting. Fibroblasts were cultured in the presence or absence of 0.3 mM CBE overnight. Next, cells were incubated with MDW933 (2 and 10 nM, for 300 min). Cells were suspended by trypsinization and analyzed by FACS using FACS Vantage (B.D. Bioscience), λ_{ex} 488 nm, λ_{em} 530 nm (bandpass filter 30 nm).

Pulse-chase experiments. Fibroblasts were cultured overnight with MDW941 (10 nM), after which they were extensively washed with PBS and incubated with MDW933 (10 nM). Cells were harvested at different time points; homogenates were prepared and subjected to SDS-PAGE. GBA labeled with MDW933 and with MDW941 were separately visualized using the Typhoon Variable Mode Imager with the above described settings.

Labeling of GBA in live mice. Experimental procedures were all approved by the appropriate ethics committee for animal experiments. C57BI/6J mice were obtained from Harlan and fed a commercially available lab diet (RMH-B; Hope Farms). Two Npc1 BALB/c WT (+/+) mice were injected intravenously via tail vein, using a restrainer with 100 µl PBS or 100 µl 100 nM MDW933 dissolved in PBS. After 2 h of administration the mice were anesthetized with FFM mix (1 ml of fentanylcitrate, 1 ml of midazalam and 2 ml of distilled water), and blood, urine and organs were collected and directly frozen in liquid nitrogen. Homogenates were made in 25 mM potassium phosphate buffer, pH 6.5, supplemented with 0.1% (v/v) Triton X-100 and labeled with MDW941 (100 nM). Homogenates were analyzed as described above.

Chaperone experiment using isofagomine. A cell line homozygous for N370S was cultured in HAMF12-DMEM medium (Invitrogen) supplied with 10% (v/v) FBS. Cells were cultured for one week with 0, 10, 30 and 300 nM isofagomine in the medium at confluency. *In vitro* activity: After one week, cells were scraped and lysed, and activity of GBA was measured at 37 °C with 4-methylumbelliferyl β-D-glucopyranoside as described above. The incubation mixture contained the corresponding concentration of isofagomine, 3 mM fluorogenic substrate, 0.2% (w/v) sodium taurocholate and 0.1% (v/v) Triton X-100 in 150 mM McIlvaine buffer, pH 5.2. For *in situ* labeling, after one week, similarly treated cells were labeled with 10 nM MDW941 for 2 h. Cells were scraped and lysed, and 25 µg of cell lysate was subjected to electrophoresis in sodium dodecylsulfate containing 7.5% polyacrylamide gels. Fluorescence of GBA labeled with MDW941 was imaged as described above and was quantified using the supplied ImageQuant software (5.1).

Received 10 May 2010; accepted 5 October 2010; published online 31 October 2010

References

1. Brady, R.O., Kanfer, J.N., Bradley, R.M. & Shapiro, D. Demonstration of a deficiency of glucocerebroside-cleaving enzyme in Gaucher's disease. *J. Clin. Invest.* **45**, 1112–1115 (1966).
2. Grabowski, G.A. Phenotype, diagnosis, and treatment of Gaucher's disease. *Lancet* **372**, 1263–1271 (2008).
3. Goker-Alpan, O. *et al.* The spectrum of Parkinsonian manifestations associated with glucocerebrosidase mutations. *Arch. Neurol.* **65**, 1353–1357 (2008).
4. Van Weely, S. *et al.* Clinical genotype of Gaucher disease in relation to properties of mutant glucocerebrosidase in cultured fibroblasts. *Biochim. Biophys. Acta* **1096**, 301–311 (1991).
5. Lachmann, R.H., Grant, I.R., Halsall, D. & Cox, T.M. Twin pairs showing discordance of phenotype in adult Gaucher's disease. *QJM* **97**, 199–204 (2004).
6. Barton, N.W. *et al.* Replacement therapy for inherited enzyme deficiency–macrophage-targeted glucocerebrosidase for Gaucher's disease. *N. Engl. J. Med.* **324**, 1464–1470 (1991).
7. Grabowski, G.A. *et al.* Enzyme therapy in type 1 Gaucher disease: comparative efficacy of mannose-terminated glucocerebrosidase from natural and recombinant sources. *Ann. Intern. Med.* **122**, 33–39 (1995).
8. Aerts, J.M., Hollak, C.E., Boot, R.G., Groener, J.E. & Maas, M. Substrate reduction therapy of glycosphingolipid storage disorders. *J. Inherit. Metab. Dis.* **29**, 449–456 (2006).
9. Platt, F.M., Neises, G.R., Dwek, R.A. & Butters, T.D. *N*-butyldeoxynojirimycin is a novel inhibitor of glycolipid biosynthesis. *J. Biol. Chem.* **269**, 8362–8365 (1994).
10. Jonsson, L.M.V. *et al.* Biosynthesis and maturation of glucocerebrosidase in Gaucher fibroblasts. *Eur. J. Biochem.* **164**, 171–179 (1987).
11. Ohashi, T. *et al.* Characterization of human glucocerebrosidase from different mutant alleles. *J. Biol. Chem.* **266**, 3661–3667 (1991).
12. Sawkar, A.R. *et al.* Gaucher disease-associated glucocerebrosidases show mutation-dependent chemical chaperoning profiles. *Chem. Biol.* **12**, 1235–1244 (2005).
13. Sawkar, A.R. *et al.* Chemical chaperones increase the cellular activity of N370S beta-glucosidase: a therapeutic strategy for Gaucher disease. *Proc. Natl. Acad. Sci. USA* **99**, 15428–15433 (2002).
14. Ron, I. & Horowitz, M. ER retention and degradation as the molecular basis underlying Gaucher disease heterogeneity. *Hum. Mol. Genet.* **14**, 2387–2398 (2005).
15. Mu, T.W. *et al.* Chemical and biological approaches synergize to ameliorate protein-folding diseases. *Cell* **134**, 769–781 (2008).
16. Steet, R.A. *et al.* The iminosugar isofagomine increases the activity of N370S mutant acid beta-glucosidase in Gaucher fibroblasts by several mechanisms. *Proc. Natl. Acad. Sci. USA* **103**, 13813–13818 (2006).
17. Yu, Z., Sawkar, A.R., Whalen, L.J., Wong, C.H. & Kelly, J.W. Isofagomine- and 2,5-anhydro-2,5-imino-D-glucitol-based glucocerebrosidase pharmacological chaperones for Gaucher disease intervention. *J. Med. Chem.* **50**, 94–100 (2007).
18. Lieberman, R.L. *et al.* Structure of acid beta-glucosidase with pharmacological chaperone provides insight into Gaucher disease. *Nat. Chem. Biol.* **3**, 101–107 (2007).
19. Kornhaber, G.J. *et al.* Isofagomine induced stabilization of glucocerebrosidase. *ChemBioChem* **9**, 2643–2649 (2008).
20. Shen, J.S., Edwards, N.J., Hong, Y.B. & Murray, G.J. Isofagomine increases lysosomal delivery of exogenous glucocerebrosidase. *Biochem. Biophys. Res. Commun.* **369**, 1071–1075 (2008).
21. Liou, B. & Grabowski, G.A. Participation of asparagine 370 and glutamine 235 in the catalysis by acid beta-glucosidase: the enzyme deficient in Gaucher disease. *Mol. Genet. Metab.* **97**, 65–74 (2009).
22. Rempel, B.P. & Withers, S.G. Covalent inhibitors of glycosidases and their applications in biochemistry and biology. *Glycobiology* **18**, 570–586 (2008).
23. Atsumi, S., Nosaka, C., Iinuma, H. & Umezawa, K. Accumulation of tissue glucosylsphingosine in Gaucher-like mouse induced by the glucosylceramidase inhibitor cyclophellitol. *Arch. Biochem. Biophys.* **304**, 302–304 (1993).
24. Hansen, F.G., Bundgaard, E. & Madsen, R. A short synthesis of (+)-cyclophellitol. *J. Org. Chem.* **70**, 10139 (2005).
25. Brumshtein, B. *et al.* Crystal structures of complexes of *N*-butyl- and *N*-nonyl-deoxynojirimycin bound to acid beta-glucosidase: insights into the mechanisms of chemical chaperone action in Gaucher disease. *J. Biol. Chem.* **282**, 29052 (2007).
26. Kacher, Y. *et al.* Acid beta-glucosidase: insights from structural analysis and relevance to Gaucher disease therapy. *Biol. Chem.* **389**, 1361–1369 (2008).
27. Overkleeft, H.S. *et al.* Generation of specific deoxynojirimycin-type inhibitors of the non-lysosomal glucosylceramidase. *J. Biol. Chem.* **273**, 26522–26527 (1998).
28. Arribas, J.C. *et al.* Differential mechanism-based labeling and unequivocal activity assignment of the two active sites of intestinal lactase/phlorizin hydrolase. *Eur. J. Biochem.* **267**, 6996–7005 (2000).
29. Aerts, J.M. *et al.* Glucocerebrosidase, a lysosomal enzyme that does not undergo oligosaccharide phosphorylation. *Biochim. Biophys. Acta* **964**, 303–308 (1988).
30. van Weely, S. *et al.* Role of pH in determining the cell-type-specific residual activity of glucocerebrosidase in type 1 Gaucher disease. *J. Clin. Invest.* **91**, 1167–1175 (1993).
31. Chang, H.H., Asano, N., Ishii, S., Ichikawa, Y. & Fan, J.Q. Hydrophilic iminosugar active-sitespecific chaperones increase residual glucocerebrosidase activity in fibroblasts from Gaucher patients. *FEBS J.* **273**, 4082–4092 (2006).
32. Rudensky, B. *et al.* Fluorescent flow cytometric assay: a new diagnostic tool for measuring beta-glucocerebrosidase activity in Gaucher disease. *Blood Cells Mol. Dis.* **30**, 97–99 (2003).
33. Gloster, T.M., Madsen, R. & Davies, G.J. Structural basis for cyclophellitol inhibition of a betaglucosidase. *Org. Biomol. Chem.* **5**, 444–446 (2007).
34. Zechel, D.L. *et al.* Iminosugar glycosidase inhibitors: structural and thermodynamic dissection of the binding of isofagomine and 1-deoxynojirimycin to beta-glucosidases. *J. Am. Chem. Soc.* **125**, 14313–14323 (2003).
35. Phenix, C.P. *et al.* Imaging of enzyme replacement therapy using PET. *Proc. Natl. Acad. Sci. USA* **107**, 10842–10847 (2010).
36. Aerts, J.M.F.G. *et al.* A procedure for the rapid purification in high yield of human glucocerebrosidase using immunoaffinity chromatography with monoclonal antibodies. *Anal. Biochem.* **154**, 655 (1986).
37. Boot, R.G. *et al.* Glucocerebrosidase genotype of Gaucher patients in The Netherlands: Limitations in prognostic value. *Hum. Mutat.* **10**, 348 (1997).
38. Andersson, U., Butters, T.D., Dwek, R.A. & Platt, F.M. *N*-butyldeoxygalactonojirimycin: a more selective inhibitor of glycosphingolipid biosynthesis than *N*-butyldeoxynojirimycin, *in vitro* and *in vivo*. *Biochem. Pharmacol.* **59**, 821 (2000).

Acknowledgments

Funding from The Netherlands Organization for Scientific Research (NWO-CW, to M.D.W., W.W.K., R.G.B., G.v.d.M., H.S.O. and J.M.F.G.A.) and The Netherlands Proteomics Centre (to B.I.F. and H.S.O.) is acknowledged.

Author contributions

M.D.W. and W.W.K. designed the experiments. M.D.W., K.-Y.L. and A.M.C.H.v.d.N. conducted the synthesis, and W.W.K. conducted the kinetic experiments and the cell assays. J.A. conducted the microscopic analysis. A.S. conducted the *in situ* assays. W.E.D.-K. conducted the *in vitro* assays. B.B. conducted the structural modeling. G.K. and B.I.F. conducted the proteomic experiments. B.H. conducted the FACS analysis. C.E.M.H. conducted the tissue culture. R.O. conducted the animal experiments. R.G.B. supervised the cell assays. G.v.d.M. supervised the synthesis. H.S.O. and J.M.F.G.A. conceived of the idea and supervised the project.

Competing financial interests

The authors declare no competing financial interests.

Additional information

Supplementary information and chemical compound information is available online at http://www.nature.com/naturechemicalbiology/. Reprints and permissions information is available online at http://npg.nature.com/reprintsandpermissions/. Correspondence and requests for materials should be addressed to J.M.F.G.A. or H.S.O.